Activation of lateral habenula inputs to the ventral midbrain promotes behavioral avoidance

Alice M Stamatakis[1] & Garret D Stuber[1,2]

Lateral habenula (LHb) projections to the ventral midbrain, including the rostromedial tegmental nucleus (RMTg), convey negative reward–related information, but the behavioral ramifications of selective activation of this pathway remain unexplored. We found that exposure to aversive stimuli in mice increased LHb excitatory drive onto RMTg neurons. Furthermore, optogenetic activation of this pathway promoted active, passive and conditioned behavioral avoidance. Thus, activity of LHb efferents to the midbrain is aversive but can also serve to negatively reinforce behavioral responding.

Neural circuits mediating reward and aversion become disrupted in neuropsychiatric diseases, such as drug addiction, anxiety disorders and depression[1,2]. Ventral tegmental area (VTA) dopamine neurons show changes in firing patterns in response to both rewarding and aversive associated stimuli[3,4]. Although dopamine neurons encode salient stimuli and predictive cues, the neural circuit elements that provide dopamine neurons with reward- and aversive-related information are not well defined. LHb neurons signal punishment and prediction errors[5]. The LHb sends excitatory projections to VTA and RMTg neurons[6–8], which can inhibit dopamine neuron output[9,10]. Although correlative evidence suggests that LHb neurons convey anti-reward and aversive information, the behavioral consequences of LHb-to-RMTg activation remain unknown. We used *ex vivo* and *in vivo* optogenetic strategies to investigate how aversive stimuli alter LHb-to-RMTg glutamatergic transmission and how direct manipulation of this pathway affects behavior.
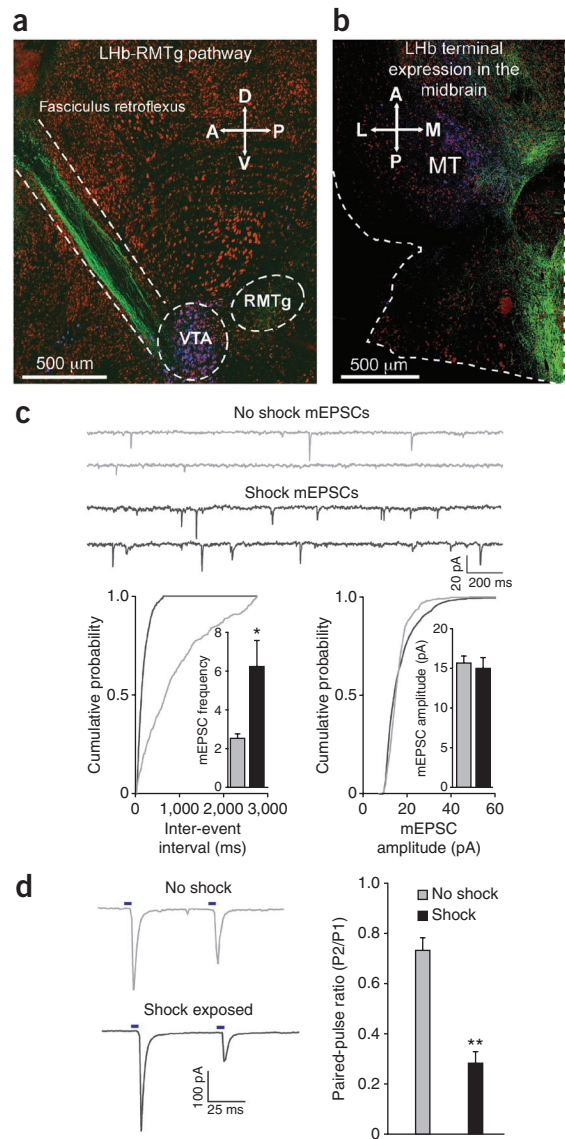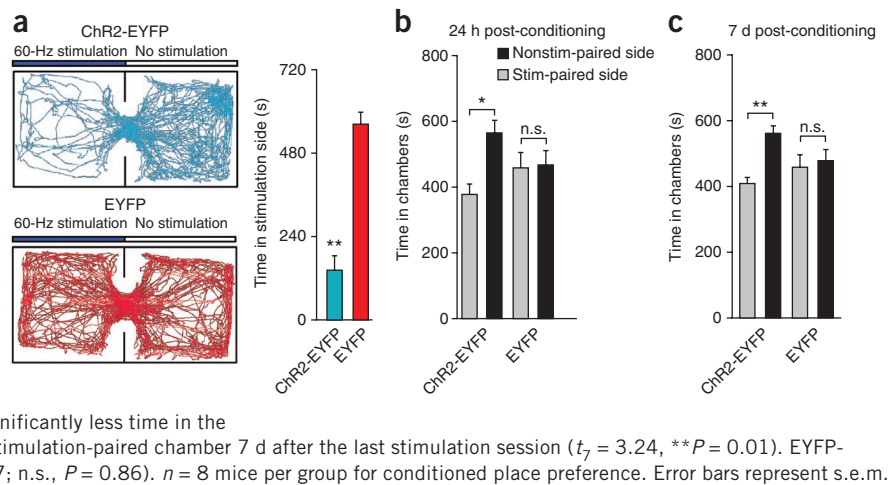

Figure 1 Acute unpredictable foot shock exposure enhances LHb-to-RMTg glutamate release. (**a**) Sagittal confocal image showing expression of ChR2-EYFP (green) in the LHb-to-midbrain pathway via the fasciculus retroflexus fiber bundle following injection of the viral construct into the LHb. Midbrain tyrosine hydroxylase–positive dopamine neurons are shown in blue. Red, neurons. A, anterior; D, dorsal; P, posterior; V, ventral. (**b**) Horizontal confocal image showing the distribution of LHb terminals in the midbrain. L, lateral; M, medial; MT, medial terminal nucleus of the accessory optic tract. (**c**) Top, representative mEPSC traces recorded from neurons from mice immediately after either 0 or 19 unpredictable foot shocks. Bottom left, representative cumulative mEPSC inter-event interval probability plot. Inset, average mEPSC frequency was significantly increased in neurons from shock-exposed mice ($t_{13} = 2.88$, $P = 0.01$). Bottom right, representative cumulative mEPSC amplitude probability plot. Inset, average mEPSC amplitude was not altered in RMTg neurons from shock-exposed mice ($t_{13} = 0.12$, $P = 0.91$). *$P < 0.05$. (**d**) Left, representative optically evoked paired-pulse ratios from LHb efferents onto RMTg neurons. Right, average paired-pulse ratios showing that paired-pulse ratios at LHb-to-RMTg synapses were significantly depressed from mice that received foot shocks ($t_{14} = 3.56$, $P = 0.003$). P1 and P2 indicate the peak currents evoked by the first and second optical pulses, respectively. $n = 8$ cells per group. **$P < 0.01$. Error bars represent s.e.m.

[1]University of North Carolina (UNC) Neurobiology Curriculum, UNC Neuroscience Center, UNC at Chapel Hill, Chapel Hill, North Carolina, USA. [2]Departments of Psychiatry & Cellular and Molecular Physiology, UNC Neuroscience Center, UNC at Chapel Hill, Chapel Hill, North Carolina, USA. Correspondence should be addressed to G.D.S. (gstuber@med.unc.edu).

Figure 2 Activation of LHb inputs to the RMTg produces passive and conditioned behavioral avoidance. (**a**) Left, real-time place-preference location plots from two representative mice showing the animal's position over the course of the 20-min session. Right, ChR2-EYFP–expressing mice spent significantly less time on the stimulated-paired side ($t_{10} = 7.90$, $P < 0.0001$). $n = 6$ mice per group for real-time place preference. **$P < 0.01$. (**b**) ChR2-EYFP–expressing mice spent significantly less time in the stimulation-paired chamber compared with the nonstimulation-paired chamber 24 h after the last stimulation conditioning session ($t_7 = 3.54$, $P = 0.01$). EYFP-expressing did not show a preference ($t_7 = 0.57$; n.s., $P = 0.58$). *$P < 0.05$. (**c**) ChR2-EYFP–expressing mice spent significantly less time in the stimulation paired chamber compared with the nonstimulation-paired chamber 7 d after the last stimulation session ($t_7 = 3.24$, **$P = 0.01$). EYFP-expressing mice did not show a preference ($t_7 = 0.17$; n.s., $P = 0.86$). $n = 8$ mice per group for conditioned place preference. Error bars represent s.e.m.

To selectively activate LHb efferents to the RMTg, we introduced channelrhodopsin-2 fused to enhanced yellow fluorescent protein (ChR2-EYFP) into the LHb of mice using viral methods (**Supplementary Fig. 1a–c**). We observed LHb terminal expression of ChR2-EYFP in midbrain structures, including the VTA and RMTg (**Fig. 1a,b** and **Supplementary Fig. 1d**). Whole-cell recordings from RMTg neurons in brain slices revealed that light pulses, which selectively stimulated LHb ChR2-expressing efferent fibers, resulted in inward currents that were blocked by the glutamatergic receptor antagonist 6,7-dinitroquinoxaline-2,3-dione (**Supplementary Fig. 1e,f**).
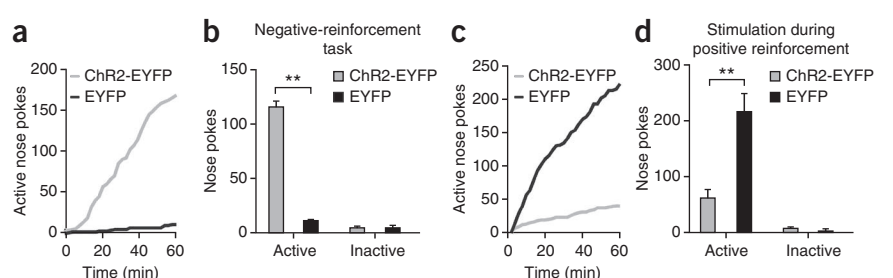
We then determined the anterior-posterior distribution of LHb-to-midbrain functional connectivity by recording from dopaminergic and nondopaminergic neurons following optical stimulation of LHb efferents in *TH-IRES-GFP* transgenic mice. Fibers originating from the LHb were predominantly localized to the posterior VTA and RMTg, and the majority of light-responsive neurons were nondopaminergic neurons located in the RMTg and posterior VTA (**Fig. 1b** and **Supplementary Fig. 1g,h**).

Given that neurotransmission by LHb neurons may encode information related to aversive stimuli processing[11], we asked whether exposure to an aversive stimulus alters excitatory neurotransmission at LHb-to-RMTg synapses. We exposed mice expressing ChR2-EYFP in LHb-to-RMTg fibers to either 0 or 19 unpredictable foot shocks in a single 20-min session. We performed whole-cell recordings 1 h later in RMTg neurons in close proximity to LHb-to-RMTg ChR2-EYFP–positive fibers. Voltage-clamp recordings from RMTg neurons from foot shock–exposed mice revealed an increase in the frequency of miniature excitatory postsynaptic currents (mEPSCs) compared

with nonshocked controls (**Fig. 1c**). Furthermore, LHb-to-RMTg glutamate release probability was significantly enhanced following shock exposure, as indexed by a reduction in the optically evoked paired pulse ratio ($P = 0.003$; **Fig. 1d**). We observed no differences in mEPSC amplitude or optically evoked AMPA/NMDA ratios, measurements of postsynaptic glutamate receptor number and function (**Fig. 1c** and **Supplementary Fig. 2**). These data suggest that aversive stimuli exposure enhances presynaptic transmission from LHb inputs to RMTg neurons.

To determine whether optogenetic stimulation of LHb-to-RMTg fibers has behavioral consequences, we optogenetically stimulated this pathway in behaving mice at 60 Hz, as this was the mean light-evoked firing rate of LHb neurons in brain slices (**Supplementary Figs. 1b,c** and **3**). To determine whether optogenetic stimulation of LHb-to-RMTg fibers resulted in passive avoidance behavior, we tested mice in a real-time place preference chamber. When an experimental mouse crossed over into a counter-balanced, stimulated-designated, contextually indistinct side of an open field, light stimulation was constantly pulsed until the mouse crossed back into the nonstimulated designated side (**Fig. 2a**). Mice expressing EYFP spent equal times on both sides of the chamber, whereas mice expressing ChR2-EYFP spent significantly less time on the stimulated side ($P < 0.0001$; **Fig. 2a** and **Supplementary Video 1**) and made significantly more escape attempts ($P = 0.018$; **Supplementary Fig. 4a**). There were no differences in total distance traveled or average velocity between ChR2-EYFP and EYFP mice across the entire session (**Supplementary Fig. 4b,c**). These data suggest that acute activation of LHb-to-RMTg fibers promotes location-specific passive avoidance behavior.

Figure 3 Activation of LHb inputs to the RMTg produces active behavioral avoidance and disrupts positive reinforcement. (**a**) Example cumulative records of active nose pokes made by a ChR2-EYFP–expressing mouse and an EYFP-expressing mouse to terminate LHb-to-RMTg optical activation. (**b**) Average number of active nose pokes from one behavioral session in following training sessions (>4 d; $t_{10} = 20.52$, $P < 0.0001$). There was no difference in inactive nose pokes between the two groups ($t_{10} = 0.29$, $P = 0.78$). $n = 6$

mice per group. **$P < 0.01$. (**c**) Example cumulative records of active nose pokes made by a ChR2-EYFP–expressing mouse and an EYFP-expressing mouse when optical stimulation was paired with the nose poke to receive a sucrose reward. (**d**) Average number of active and inactive nose pokes during positive reinforcement ($t_{14} = 4.01$, **$P < 0.01$). There was no difference in inactive nose pokes between the two groups ($t_{14} = 1.22$, $P = 0.24$). $n = 8$ mice per group. Error bars represent s.e.m.

Although activation of the LHb-to-RMTg pathway induced acute avoidance, we next determined if activation of this pathway produced conditioned avoidance using a standard nonbiased conditioned place preference procedure. ChR2-EYFP-expressing mice showed a significant conditioned place aversion for the stimulation-paired chamber 24 h after the last conditioning session, where optogenetic stimulation was paired with a distinct context, whereas the EYFP-expressing mice showed no preference or aversion (**Fig. 2b**). This conditioned place aversion was maintained in the ChR2-EYFP–expressing mice 7 d after the last conditioning session (**Fig. 2c**), indicating that activity in this pathway also promotes conditioned avoidance.

To determine whether mice would perform an operant response to actively avoid activation of LHb-to-RMTg fibers, we placed ChR2-EYFP– or EYFP-expressing mice in chambers in which they could nose poke to terminate optogenetic stimulation of LHb-to-RMTg fibers (**Supplementary Fig. 5a**). ChR2-EYFP–expressing mice learned to nose poke to terminate laser stimulation over three daily training sessions (**Supplementary Fig. 6**). Following training, ChR2-EYFP–expressing mice made significantly more active nose pokes to terminate LHb-to-RMTg activation than did EYFP-expressing mice ($P < 0.0001$; **Fig. 3a**–**c**), resulting in a significant increase in the percentage of time the stimulation was off (percent time stimulation was off: ChR2-EYFP, $47.5 \pm 7.1\%$; EYFP, $2.8 \pm 0.9\%$; $t_{10} = 6.28$, $P < 0.0001$). These data suggest that LHb-to-RMTg activity can negatively reinforce behavioral responding.

Next, we examined whether LHb-to-RMTg activation disrupts positive reinforcement. We trained a separate group of mice to nose poke to earn liquid sucrose rewards. Following stable responding, nose pokes to earn sucrose in subsequent test sessions were paired with a 2-s, 60-Hz LHb-to-RMTg stimulation (**Supplementary Fig. 5b**). ChR2-EYFP–expressing mice receiving stimulations made significantly fewer nose pokes than EYFP-expressing mice and took significantly longer to retrieve and consume the rewards ($P < 0.01$; **Fig. 3c,d**, **Supplementary Fig. 7** and **Supplementary Video 2**). Notably, there were no significant differences between the two groups in the prior session, in which nose pokes were not paired with LHb-to-RMTg stimulation ($t_{14} = 1.64$, $P = 0.12$), suggesting that stimulation of this pathway time-locked to an operant response serves as a punishment.

We found that activation of LHb terminals in the RMTg promotes active, passive and conditioned behavioral avoidance, suggesting that endogenous activity of LHb glutamatergic inputs to the RMTg conveys information related to aversion. Our data suggest that the LHb's connection with midbrain GABA neurons is crucial for promoting these behaviors. Consistent with this, direct excitation of VTA GABA neurons disrupts reward-related behaviors[10] and stimulation of VTA GABA neurons or inhibition of VTA dopamine neurons promotes aversion[12]. Notably, optogenetic stimulation of LHb terminals in the RMTg suppressed positive reinforcement and supported negative reinforcement, indicating that this pathway can bidirectionally affect the same behavioral response (nose poking) depending on the task.

Dopamine signaling in the nucleus accumbens promotes positive reinforcement[2,3]. Thus, motivated behavior to suppress activation of the LHb-to-RMTg pathway may also depend on dopamine signaling in the nucleus accumbens. Although encoding negative consequences requires multiple neural circuits, activation of glutamatergic presynaptic inputs to the LHb[13,14] or LHb inputs to the midbrain alone produces aversion. Given that LHb projections are phylogenetically well conserved[15], neurotransmission in this pathway is likely to be essential for survival by promoting learning and subsequent behavior to avoid stimuli associated with negative consequence.

METHODS
Methods and any associated references are available in the online version of the paper.

Note: Supplementary information is available in the online version of the paper.

AUTHOR CONTRIBUTIONS
A.M.S. collected all of the data. A.M.S. and G.D.S. designed the experiments, analyzed the data and wrote the manuscript.

COMPETING FINANCIAL INTERESTS
The authors declare no competing financial interests.

Published online at http://www.nature.com/doifinder/10.1038/nn.3145.
Reprints and permissions information is available online at http://www.nature.com/reprints/index.html.

1. Shin, L.M. & Liberzon, I. *Neuropsychopharmacology* **35**, 169–191 (2010).
2. Koob, G.F. & Volkow, N.D. *Neuropsychopharmacology* **35**, 217–238 (2010).
3. Schultz, W., Dayan, P. & Montague, P.R. *Science* **275**, 1593–1599 (1997).
4. Brischoux, F., Chakraborty, S., Brierley, D.I. & Ungless, M.A. *Proc. Natl. Acad. Sci. USA* **106**, 4894–4899 (2009).
5. Bromberg-Martin, E.S. & Hikosaka, O. *Nat. Neurosci.* **14**, 1209–1216 (2011).
6. Jhou, T.C., Fields, H.L., Baxter, M.G., Saper, C.B. & Holland, P.C. *Neuron* **61**, 786–800 (2009).
7. Perrotti, L.I. *et al. Eur. J. Neurosci.* **21**, 2817–2824 (2005).
8. Matsui, A. & Williams, J.T. *J. Neurosci.* **31**, 17729–17735 (2011).
9. Ji, H. & Shepard, P.D. *J. Neurosci.* **27**, 6923–6930 (2007).
10. van Zessen, R., Phillips, J.L., Budygin, E.A. & Stuber, G.D. *Neuron* **73**, 1184–1194 (2012).
11. Matsumoto, M. & Hikosaka, O. *Nat. Neurosci.* **12**, 77–84 (2009).
12. Tan, K.R. *et al. Neuron* **73**, 1173–1183 (2012).
13. Li, B. *et al. Nature* **470**, 535–539 (2011).
14. Shabel, S.J., Proulx, C.D., Trias, A., Murphy, R.T. & Malinow, R. *Neuron* **74**, 475–481 (2012).
15. Stephenson-Jones, M., Floros, O., Robertson, B. & Grillner, S. *Proc. Natl. Acad. Sci. USA* **109**, E164–E173 (2012).

ONLINE METHODS

Experimental subjects and stereotaxic surgery. We grouped housed adult (25–30 g) male C57BL/6J mice (Jackson Laboratory) until surgery. We anesthetized the mice with ketamine (150 mg per kg of body weight) and xylazine (50 mg per kg) and placed the mice in a stereotaxic frame (Kopf Instruments). We bilaterally microinjected 0.4 μl of purified and concentrated adeno-associated virus (~10^{12} infections units per ml, packaged and titered by the UNC Vector Core Facility) into the LHb (coordinates from bregma: −1.7 anterior/posterior, ±0.48 medial/lateral, −3.34 dorsal/ventral). LHb neurons were transduced with virus encoding ChR2-EYFP or EYFP under the control of the human synapsin (*SYN1*) promoter. Following surgery, we individually housed the mice. For behavioral experiments, we also implanted mice with a unilateral chronic fiber directed above the RMTg (coordinates from bregma: −3.9 AP, ±0.3 ML, −4.8 DV). We performed all experiments 6–8 weeks after surgery. We conducted all procedures in accordance with the Guide for the Care and Use of Laboratory Animals, as adopted by the US National Institutes of Health, and with approval of the UNC Institutional Animal Care and Use Committees.

Histology, immunohistochemistry and microscopy. We anesthetized mice with pentobarbital and killed them by perfusion with phosphate-buffered saline followed by 4% paraformaldehyde (wt/vol) in phosphate-buffered saline. We subjected 40-μm brain sections to immunohistochemical staining for neuronal cell bodies and/or tyrosine hydroxylase (Pel Freeze, made in sheep; Neurotrace: Invitrogen, 640-nm excitation/660-nm emission or 435-nm excitation/455-nm emission) as previously described[10]. We mounted sections and captured *z* stack and tiled images on a Zeiss LSM Z10 confocal microscope using a 20× or 63× objective. For determination of optical fiber placements, we imaged tissue at 10× on an upright fluorescent microscope. We recorded optical stimulation sites as the location in tissue where visible optical fiber tracks terminated.

Slice preparation for patch-clamp electrophysiology. We prepared brain slices for patch-clamp electrophysiology as previously described[10,16]. Briefly, we anesthetized mice with pentobarbital and perfused transcardially with modified artificial cerebrospinal fluid. We then rapidly removed the brains and placed them in the same solution that we used for perfusion at ~0° C. We cut sagittal midbrain slices containing the RMTg (200 μm) or horizontal midbrain slices containing the VTA and RMTg (200 μm) on a vibratome (VT-1200, Leica Microsystems), placed the slices in a holding chamber and allowed them to recover for at least 30 min before recording.

Patch-clamp electrophysiology. We made whole-cell voltage-clamp recordings of RMTg neurons as previously described[16]. Briefly, we back-filled patch electrodes (3.0–5.0 MΩ) for current-clamp recordings, with a potassium-gluconate internal solution[10]. For voltage-clamp recordings, we back-filled patch electrodes with a cesium methanesulfonic acid internal solution[17]. For optical stimulation of EPSCs, we used light pulses from an LED coupled to a 40× microscope objective (1-ms pulses of 1–2 mW, 473 nm) to evoke presynaptic glutamate release from LHb projections to RMTg. For mEPSCs and optically evoked EPSCs, we voltage-clamped RMTg neurons at −70 mV. For AMPA and NMDA receptor experiments, the holding potential was +40 mV. We added picrotoxin (100 mM) to the external solution to block GABA$_A$ receptor–mediated inhibitory postsynaptic currents for all experiments. For mEPSCs, we added tetrodotoxin (500 nM) to the external solution to suppress action potential driven release. We calculated the AMPA/NMDA ratio and paired pulse ratio as previously described[18]. We averaged six sweeps together to calculate both the AMPA/NMDA ratio and the paired pulse ratio. We collected mEPSCs for 5 min or until 300 mEPSCs were collected. To determine where, anterior-posterior, midbrain neurons were light responsive, we injected *TH-IRES-GFP* mice with *SYN1-ChR2-EYFP* into the LHb. We voltage-clamped (−70mV) GFP-positive (tyrosine hydroxylase positive) and GFP-negative (tyrosine hydroxylase negative) midbrain neurons and categorized the cells as light-responsive if a light pulse resulted in an average evoked current across six sweeps of >20 pA.

Shock procedure for patch-clamp electrophysiology. We placed mice expressing ChR2-EYFP in the LHb-to-RMTg pathway into standard mouse behavioral chambers (Med Associates) equipped with a metal grid floor capable of delivery foot shocks for 20 min. Mice received either 19 or 0 unpredictable foot shocks (0.75 mA, 500 ms). We presented shocks with a pseudo-random interstimulus interval of 30, 60 or 90 s. We anesthetized mice for patch-clamp electrophysiology 1 h after the session ended (described above).

In vivo optogenetic excitation. For all behavioral experiments, we injected mice with a ChR2-EYFP or EYFP virus and implanted them with a chronic unilateral custom-made optical fiber targeted to the RMTg as described previously[19]. We connected mice to a 'dummy' optical patch cable 3 d before the experiment each day for 30–60 min to habituate them to the tethering procedure. Following the tethering procedure, we then ran mice in the behavioral procedures (see below). We used a 10-mW laser with a stimulation frequency of 60 Hz and a 5-ms light pulse duration for all behavioral experiments.

Real-time place preference. We placed mice in a custom-made behavioral arena (50 × 50 × 25 cm black plexiglass) for 20 min. We assigned one counterbalanced side of the chamber as the stimulation side. We placed the mouse in the non-stimulated side at the onset of the experiment and delivered a 60-Hz constant laser stimulation each time the mouse crossed to the stimulation side of the chamber until the mouse crossed back into the nonstimulation side. We recorded behavioral data via a CCD camera interfaced with Ethovision software (Noldus Information Technologies). We defined an escape attempt as each time a mouse attempted to climb out of the apparatus. We only scored an attempt if no paws were on the ground.

Conditioned place preference. The conditioned place preference apparatus (Med Associates) consisted of a rectangular cage with a left black chamber (17 cm × 12.5 cm) with a vertical metal bar floor, a center gray chamber (15 cm × 9 cm) with a smooth gray floor and a right white chamber (17 cm × 12.5 cm) with a wire mesh floor grid. We monitored mouse location in the chamber using a computerized photo-beam system. The conditioned place preference test consisted of 4 d. Day 1 consisted of a preconditioning test that ensured that mice did not have a preference for one particular side[20]. On days 2 and 3, we placed the mice into either the black or white side of the chamber (counterbalanced across all mice) and delivered either 0.5 s of 60-Hz stimulation with an interstimulus interval of 1 s for 20 min, or no stimulation. Approximately 4 h later, we placed the mice into the other side of the chamber and the mice received the other treatment. We placed the mice back into the chamber 24 h after the last conditioning session with all three chambers accessible to assess preference for the stimulation and nonstimulation paired chambers. To assess long-term associations between the stimulation and context, we placed the mice back in the chambers 7 d later.

Negative and positive reinforcement procedures. Behavioral training and testing occurred in mouse operant chambers interfaced with optogenetic stimulation equipment as described previously[1]. For the negative reinforcement procedure, we placed mice into the chamber and delivered 500 ms of 60-Hz optical stimulation with an interstimulus interval of 1 s. We trained mice on a fixed ratio (FR1) training schedule, in which each nose poke resulted in 1 20-s period in which the laser was shut off and the LHb-to-RMTg pathway was not optogenetically activated. In addition, a tone and houselight cue turned on for the entire 20 s and turned off when the laser stimulation returned. For the positive reinforcement procedure, we food restricted a separate group of mice to 90% of their free-feeding bodyweight. We then trained mice for one session per day for 1 h in the operant chambers on a FR1 schedule (in which each nose poke resulted in 20 μl of a 15% sucrose solution, wt/vol). In addition, a tone and houselight cue turned on for 2 s. Once the mice reached stable behavioral responding (as determined by 3 d of over 100 active nose pokes that did not vary by more than 20% from the first of the 3 d), mice received 2 s of 60-Hz optical stimulation time-locked to the cue following each active nose poke. For both behaviors, we recorded inactive nose pokes, but these had no programmed consequences. In addition, we collected and time-stamped the number of active and inactive nose pokes.

Data analysis. We used *t* tests and one- or two-way analyses of variance to analyze all behavioral and electrophysiological data when applicable. When we obtained significant main effects, we performed Tukey's HSD *post hoc* tests for group comparison. For all behavioral experiments, we analyzed the

data in Ethovision, Matlab, Excel and Prism. We used six mice per group for the real-time place preference and negative reinforcement experiments and eight mice per group for the conditioned place preference and positive reinforcement experiments. We used no more than two neurons from a given animal for patch-clamp electrophysiology in the aversive stimuli exposure experiments.

16. Stuber, G.D. *et al. Nature* **475**, 377–380 (2011).
17. Stuber, G.D., Hnasko, T.S., Britt, J.P., Edwards, R.H. & Bonci, A. *J. Neurosci.* **30**, 8229–8233 (2010).
18. Stuber, G.D. *et al. Alcohol. Clin. Exp. Res.* **32**, 1714–1720 (2008).
19. Sparta, D.R. *et al. Nat. Protoc.* **7**, 12–23 (2012).
20. Cunningham, C.L., Gremel, C.M. & Groblewski, P.A. *Nat. Protoc.* **1**, 1662–1670 (2006).